112 J. Chem. Eng. Data 1981, 26, 112-115

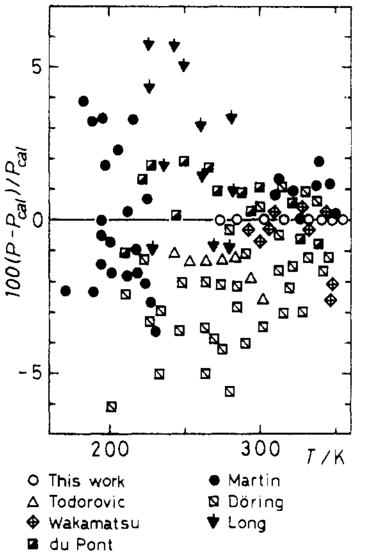

Figure 2. Comparison of experimental vapor pressures with eq 1.

Acknowledgment

We are greatly indebted to Mitsui Fluorochemicals, Co., Ltd., Tokyo, for kindly furnishing the sample of R502. We are also grateful to the National Research Laboratory of Metrology, Ibaraki, for their calibration of the thermometer. H. Kobayashi and M. Suzuki have provided valuable assistance in the experiments.

Glossary

A, B, C	coefficients in eq 1
P	pressure in MPa
P_c	critical pressure in MPa
P_s	vapor pressure in MPa
P_0	coefficients in eq 1
T	temperature in K
T_c	critical temperature in K
T_0	coefficients in eq 1
Z	compressibility factor

Greek Letters

ρ	density in kg/m^3
ρ_c	critical density in kg/m^3

Literature Cited

(1) Martin, J. J.; Downing, R. C., *ASHRAE Trans.* **1970**, *76*, 129.
(2) Todorović, M.; Saopštenja, Termotehnika Institut, Mašinskog Fakulteta, University of Belgrade, Belgrade, Yugoslavia, 2, 1971.
(3) Döring, R. *Proc. Int. Inst. Refrig., 14th* **1975**, 196.
(4) Wakamatsu, S. MS Thesis, Faculty of Engineering, Tokyo Metropolitan University, Tokyo, Japan, 1976.
(5) Long, L. J., cited in ref *1*.
(6) E. I. du Pont de Nemours and Co., cited in ref. *1*.
(7) Watanabe, K.; Tanaka, T.; Oguchi, K. *Proc. Symp. Thermophys. Prop., 7th* **1977**, 470.
(8) CODATA Task Group on Key Values for Thermodynamics, *CODATA Bull.* **1977**, *No. 22*.
(9) Badylkes, I. S. *Kholod. Tekh.* **1964**, 41-5, 41.
(10) Löffler, H. J. *Kältetechnik* **1967**, *19*, 201.
(11) Todorović, M. *Klimat. Grej.-Hlad.* (*YU.*) **1972**, *1*, 2.

Received for review February 26, 1980. Accepted November 10, 1980. Financial support was provided by the Fukuzawa Memorial Research Fund of Keio University.

Equilibrium Adsorption of Oxygen, Nitrogen, Carbon Monoxide, and Their Binary Mixtures on Molecular Sieve Type 10X

John T. Nolan, Thomas W. McKeehan, and Ronald P. Danner*

Department of Chemical Engineering, The Pennsylvania State University, University Park, Pennsylvania 16802

Pure-gas adsorption isotherms of oxygen, nitrogen, and carbon monoxide on molecular sieve type 10X have been determined at 32, −50, and −150 °F. Binary adsorption data for all pairs of these adsorbates on the same adsorbent have been collected at the same temperatures and a pressure of 760 mmHg.

Introduction

Adsorption data for the oxygen–nitrogen–carbon monoxide system on molecular sieve type 10X have been reported previously from our laboratory. Danner and Wenzel (*1*) provided the pure-component isotherms at −200 °F and the binary-mixture data at the same temperature and 760 mmHg. All of these data were collected on adsorbent samples taken from the same batch of adsorbent and thus provide the most comprehensive data set available in the literature on gas-mixture adsorption equilibria.

Experimental Section

Experimental Apparatus. The apparatus used was of the volumetric type. The total quantity of each gas admitted to the system and the amount of each gas in the vapor remaining after adsorption equilibrium was established were determined by appropriate $P-V-T$ measurements and analysis by a gas chromatograph. The adsorbed-phase parameters were determined by the difference between the quantities of admitted and remaining gases. In the case of gas-mixture studies, the vapor phase was recycled through the adsorbent bed in order to obtain equilibrium.

The temperature was measured with a copper–constantan thermocouple which had been calibrated with a certified platinum resistance thermometer. Pressures were read from a 60-in., U-type mercury manometer. The estimated accuracies are ±0.2 °F, ±0.3 mmHg, and ±0.5% for the total volume adsorbed and ±0.6 mol % for the phase compositions. Details of the equipment and the operating procedures are described in the previous publication of Dorfman and Danner (*2*).

Materials. The adsorbent used was Linde molecular sieve type 10X in the form of $^1/_{16}$-in. diameter pellets of $\sim ^1/_4$-in. length. The adsorbent pellets were a mixture of 80% crystalline zeolites with 20% inert clay bonding material. This is the same batch of sieves used for the previously reported data (*1*, *2*). The nitrogen isotherm data given in Table I at liquid-nitrogen temperature (−318.7 °F) agree within 2% with the data reported by Danner (*3*). From these data the surface area of this adsorbent was calculated by the n-layer BET method (*4*) to be 672 m^2/gm. Before the adsorbent was weighed into the sample holder, it was regenerated at 600 °F under a vacuum of 50 μmHg for a period of more than 12 h. Between adsorption runs

0021-9568/81/1726-0112$01.25/0 © 1981 American Chemical Society

Table I. Pure-Gas Adsorption Data

oxygen		nitrogen		carbon monoxide		oxygen		nitrogen		carbon monoxide	
P, mmHg	V_a, cm^3 STP/g	P, mmHg	V_a, cm^3 STP/g	P, mmHg	V_a, cm^3 STP/g	P, mmHg	V_a, cm^3 STP/g	P, mmHg	V_a, cm^3 STP/g	P, mmHg	V_a, cm^3 STP/g
$T = -150$ °F											
52.6	7.5	9.9	15.4	4.3	21.5	585.5	42.1	720.0	70.9	887.2	96.2
125.4	13.8	53.1	28.8	18.7	42.0	686.2	47.0	967.1	76.2	997.5	97.8
207.1	19.8	124.7	40.5	78.2	59.3	800.0	52.4	1231.7	80.3	1220.1	100.5
291.9	25.4	229.4	50.4	197.8	73.2	938.1	58.1	1485.6	83.4	1522.3	103.3
392.5	31.5	360.2	58.4	379.9	83.6	1075.9	62.2	1697.8	85.7	1737.8	104.9
487.4	36.9	529.6	65.3	614.1	90.9	1223.8	68.0	1896.1	87.3	1981.3	106.6
$T = -50$ °F											
16.7	0.2	21.5	3.4	2.5	1.1	796.4	9.9	898.1	27.2	398.3	36.0
28.6	0.4	41.0	5.1	3.3	2.9	846.8	10.3	948.4	28.4	448.2	37.2
43.0	0.6	64.2	6.7	4.8	5.1	897.3	11.0	999.5	28.8	498.2	39.0
54.6	0.8	91.3	8.2	5.1	7.3	945.9	11.4	1047.6	29.9	547.8	40.2
81.7	1.1	121.7	9.7	7.1	7.3	995.7	12.0	1097.4	30.2	597.6	41.5
83.2	1.2	149.5	10.7	12.4	9.4	1046.8	12.5	1147.7	31.1	647.2	42.7
108.5	1.5	169.2	11.4	16.4	10.4	1096.4	13.1	1195.5	31.4	694.5	43.7
109.0	1.5	198.3	12.3	21.8	11.4	1145.7	13.4	1245.8	32.3	745.1	44.9
136.8	1.9	198.5	12.6	29.3	12.9	1196.3	14.1	1296.2	32.7	798.2	45.8
151.8	2.1	246.8	14.1	34.7	13.4	1244.3	14.5	1344.5	33.5	847.0	46.8
186.7	2.6	299.2	15.3	40.5	14.3	1295.4	15.1	1395.6	33.8	895.6	47.6
249.6	3.4	346.0	16.8	48.3	15.3	1344.0	15.4	1446.7	34.7	945.4	48.5
300.0	4.1	397.6	17.8	56.2	16.1	1396.8	16.1	1495.0	34.9	995.7	49.3
350.3	4.7	448.4	19.3	74.1	17.9	1443.4	16.4	1543.8	35.7	1044.8	50.1
398.8	5.3	497.0	20.1	93.3	19.7	1494.7	17.0	1593.1	36.3	1095.4	51.0
450.9	5.9	549.3	21.5	117.6	21.8	1545.8	17.4			1144.9	51.4
498.5	6.4	596.6	22.0	146.9	23.8	1593.1	18.0			1195.0	52.3
549.1	7.0	648.7	23.4	175.8	25.6					1295.7	53.5
598.9	7.6	698.8	24.0	200.3	27.1					1394.3	54.7
647.7	7.9	747.9	25.2	249.1	29.6					1493.4	55.8
695.8	8.8	797.4	25.7	298.7	31.9					1593.9	56.8
746.3	9.3	848.0	26.9	339.4	33.5						
$T = 32$ °F											
49.6	0.22	10.1	0.30	2.0	0.38	697.0	3.21	746.6	10.28	496.7	17.98
60.7	0.27	18.2	0.52	4.1	0.99	746.3	3.47	796.7	10.75	542.2	18.83
71.3	0.33	27.1	0.75	7.8	1.78	798.7	3.67	846.2	11.20	597.1	19.56
71.6	0.31	40.5	1.11	13.7	2.72	845.7	3.94	896.1	11.61	645.4	20.45
79.9	0.37	49.8	1.30	22.8	3.72	895.6	4.08	946.4	12.04	697.3	21.08
90.0	0.41	74.9	1.82	29.8	4.29	945.9	4.35	996.2	12.29	746.9	21.90
100.9	0.47	90.8	2.18	37.7	5.68	995.5	4.50	1046.3	12.69	797.2	22.42
115.6	0.52	101.2	2.29	38.4	4.98	1044.5	4.77	1096.9	13.19	846.2	23.19
140.6	0.65	149.2	3.15	52.9	6.60	1094.9	5.05	1145.9	13.56	898.1	23.73
149.5	0.67	199.0	4.02	69.0	7.45	1144.9	5.21	1194.8	13.92	945.9	24.42
199.3	0.93	245.6	4.63	83.7	8.20	1195.0	5.44	1196.3	13.97	996.5	24.89
248.6	1.14	299.7	5.37	99.9	8.81	1245.6	5.60	1244.3	14.31	1045.3	25.61
298.7	1.39	349.3	6.01	129.0	9.89	1294.4	5.80	1294.9	14.67	1095.1	26.13
347.0	1.61	398.3	6.60	145.9	10.47	1343.5	5.99	1347.3	15.05	1194.8	27.16
398.1	1.83	446.6	7.17	201.6	12.03	1395.3	6.25	1394.3	15.36	1294.4	28.15
448.2	2.06	498.0	7.76	228.1	12.65	1442.9	6.42	1443.1	15.62	1397.3	29.16
497.2	2.31	547.6	8.25	298.7	14.31	1495.0	6.67	1493.7	15.98	1443.4	29.52
547.6	2.52	597.4	8.76	347.3	15.32	1542.8	6.84	1543.3	16.41	1493.7	30.05
597.4	2.81	645.4	9.31	398.1	16.26	1593.1	7.05	1593.6	16.69	1541.8	30.41
646.7	2.97	697.0	9.80	446.9	17.24						
Nitrogen at -318.7 °F											
1.8	92.4	89.3	161.3	298.9	165.8	26.3	157.2	172.2	163.7	497.2	168.9
2.3	139.9	112.3	162.1	299.5	165.8	38.4	158.5	203.6	164.2	497.7	168.6
2.8	147.4	122.4	162.4	397.6	167.4	58.7	160.0	247.6	165.1	591.3	171.2
2.8	148.8	123.9	162.0	400.6	167.3	80.4	160.9	253.4	165.1	597.9	170.2
22.8	156.7	152.3	163.2	474.7	169.4						

the sieve was regenerated in situ overnight at a vacuum of less than 25 μmHg and a temperature of 250 °F.

Pure-Component Data

The isotherm data collected for oxygen, nitrogen, and carbon monoxide on molecular sieve type 10X at 32, −50, and −150 °F are listed in Table I. Isobars at 760 mmHg obtained from these data and those of Danner and Wenzel (*1*) at −200 °F are shown in Figure 1. In general, the adsorptive capacity increases in the order oxygen, nitrogen, carbon monoxide, and the capacities increase as the temperature decreases. The adsorbed volume of oxygen, however, increases more sharply than the other two gases as the temperature decreases, so that the isobar of oxygen crosses the isobar of nitrogen at −195 °F. Extrapolation indicates that the oxygen isobar crosses the carbon monoxide isobar at ca. −210 °F. These isobar crossings are not surprising since oxygen has the highest normal boiling point (−297.3 °F) compared to carbon monoxide (−312.6 °F) and nitrogen (−320.5 °F).

The isotherms all exhibited behavior characteristic of the Langmuir type, i.e., isotherms that can be described by eq 1.

$$P/V_a = 1/bV_m + P/V_m \qquad (1)$$

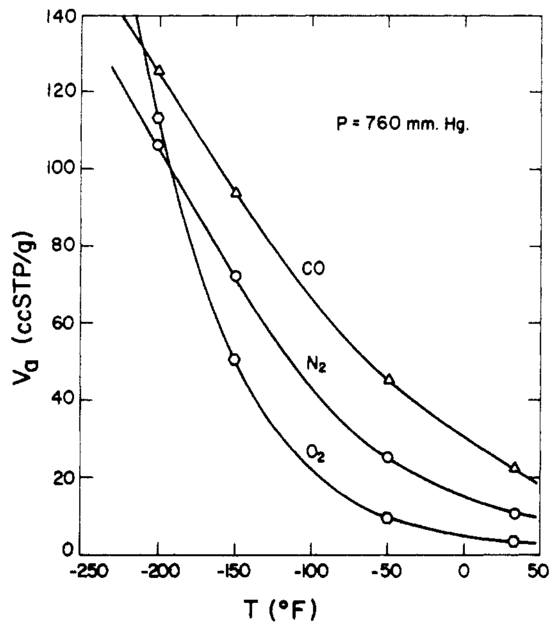

Figure 1. Isobars for adsorption of pure gases on molecular sieve type 10X.

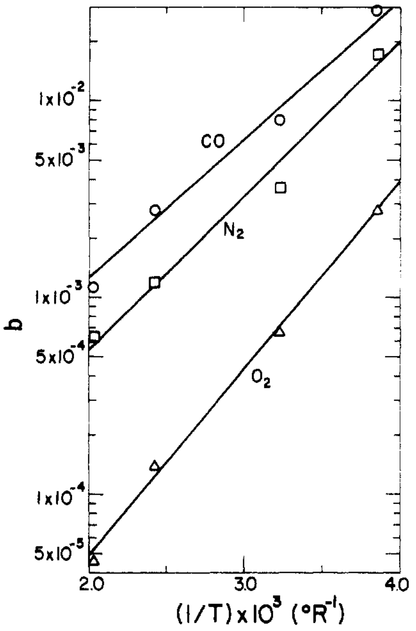

Figure 2. Temperature dependence of Langmuir equation energy parameter.

Plots of P/V_a as a function of pressure were generally linear over a large portion of the pressure range, although in all cases nonlinearity was observed in the low-pressure region. The Langmuir theory predicts that the energy parameter, b, should be related to temperature such that a plot of log b vs. $1/T$ is linear. Figure 2 shows that this behavior was closely approximated for each of the three gases at the four temperatures available. This then is at least an elementary check on the internal consistency of the isotherm data.

Gas-Mixture Data

In Table II the vapor and adsorbed-phase compositions and total volumes adsorbed are given for the three binary mixtures at the three temperatures. Figures 3 and 4 show the temperature behavior of the oxygen–carbon monoxide and nitrogen–carbon monoxide adsorption phase equilibria diagrams. The -200 °F lines of Danner and Wenzel (1) have been in-

Table II. Gas-Mixture Adsorption Data

X_1	Y_1	V_a	X_1	Y_1	V_a
$T = -150$ °F, $P = 760$ mmHg					
O_2 (1)–N_2 (2)					
0	0	71.7	31.2	69.7	65.9
6.1	18.5	70.8	42.9	83.2	62.7
15.6	42.3	69.3	54.9	91.6	59.2
20.1	51.7	68.6	70.6	97.0	54.8
26.3	62.8	67.3	89.0	99.5	52.9
N_2 (1)–CO (2)					
5.7	25.6	90.6	26.8	72.6	83.7
12.4	46.9	87.8	30.2	79.1	81.9
14.4	49.8	88.1	34.5	82.7	80.9
19.2	62.1	85.3	49.3	90.9	78.1
25.0	72.4	83.4	72.9	97.1	74.3
O_2 (1)–CO (2)					
5.1	28.6	92.0	16.3	68.9	85.7
6.8	36.6	90.7	17.3	72.8	84.0
8.0	43.0	89.1	19.9	77.7	83.6
8.6	43.4	90.0	20.8	79.8	82.0
10.3	50.6	89.0	23.8	83.1	80.0
11.9	56.2	88.2	36.2	93.6	72.4
13.6	62.4	86.3	53.4	98.7	63.6
15.4	67.7	85.1	74.2	99.4	56.4
$T = -50$ °F, $P = 760$ mmHg					
O_2 (1)–N_2 (2)					
1.0	4.7	24.1	32.0	75.1	16.3
3.0	13.3	23.7	41.8	83.5	14.5
6.3	26.9	22.5	57.5	91.4	12.4
10.7	39.1	21.3	70.8	96.1	10.9
12.8	44.8	20.6	77.7	96.7	10.4
22.0	65.0	18.2	91.6	98.7	9.4
31.3	78.0	16.4			
N_2 (1)–CO (2)					
1.3	6.1	43.7	31.5	78.6	33.7
3.5	15.1	42.8	36.6	84.1	32.6
5.9	24.6	41.8	41.2	87.3	31.7
10.3	39.9	39.9	43.1	86.9	31.2
18.2	58.5	37.3	62.5	94.8	27.8
20.6	61.0	36.8	85.9	98.5	25.8
25.7	69.9	35.5	95.9	99.2	25.5
O_2 (1)–CO (2)					
0.5	4.1	43.3	15.4	78.5	29.6
1.5	11.6	42.4	18.2	83.4	27.6
2.7	21.4	41.3	44.8	96.0	15.5
5.2	37.9	39.0	56.3	97.7	13.2
7.2	49.4	36.7	66.4	98.9	11.7
9.4	58.9	34.6	73.9	99.0	11.0
12.5	69.8	31.9	89.8	99.7	9.7
$T = 32$ °F, $P = 760$ mmHg					
O_2 (1)–N_2 (2)					
2.0	3.5	10.4	23.0	59.6	7.4
3.4	14.6	9.6	29.7	68.4	6.9
3.5	9.7	10.1	40.0	79.4	5.8
11.8	35.9	8.7	56.3	89.0	5.0
16.7	47.7	8.3	76.3	95.0	4.0
22.3	57.8	7.4			
N_2 (1)–CO (2)					
0.9	4.0	21.2	44.2	84.3	13.9
9.9	32.8	19.2	50.6	88.5	13.3
16.8	50.5	17.6	52.0	89.0	13.4
23.6	63.2	16.5	57.6	92.2	12.8
30.2	71.7	15.7	58.4	92.4	12.8
33.6	74.9	14.9	64.4	93.8	12.3
36.9	77.8	14.9	68.8	95.9	12.1
42.1	83.2	14.4	72.6	96.8	11.9
O_2 (1)–CO (2)					
1.7	8.2	20.7	30.2	92.1	9.3
4.0	27.8	18.8	33.7	94.6	8.6
8.3	51.1	16.3	39.4	96.2	7.2
14.1	71.0	13.6	52.0	98.4	5.8
20.1	83.2	11.6	63.5	98.7	5.0
25.2	89.2	10.3	78.5	99.2	4.1

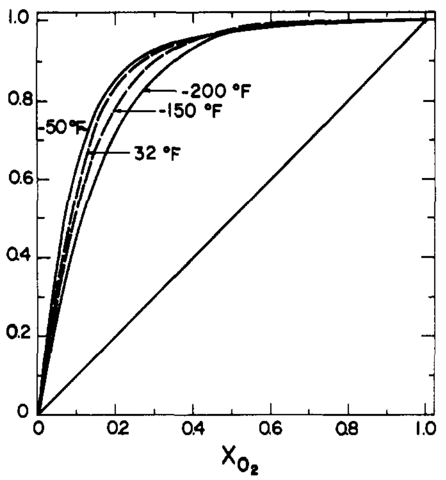

Figure 3. Adsorption phase diagram for oxygen-carbon monoxide mixtures on molecular sieve type 10X at 760 mmHg.

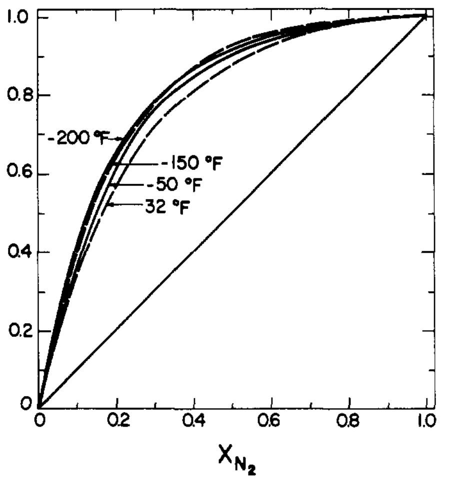

Figure 4. Adsorption phase diagrams for nitrogen-carbon monoxide mixtures on molecular sieve type 10X at 760 mmHg.

cluded in these figures. In order to make the figures reasonably clear, the data points had to be deleted. The temperature dependency of the adsorption phase diagrams is not particularly strong. The oxygen-nitrogen diagram is not shown, but it looks quite similar to the oxygen-carbon monoxide figure.

The oxygen-nitrogen and oxygen-carbon monoxide systems both show decreasing extent of separation (curves closer to the 45° line) with decreasing temperature. In both cases the more volatile component is more strongly adsorbed (i.e., nitrogen and carbon monoxide). In vapor-liquid equilibrium, oxygen would be the rich component in the condensed phases of both binary systems. The observed temperature behavior is the result of complex interplay between adsorbent-adsorbate interactions and adsorbate-adsorbate interactions. One can speculate that, as the temperature is lowered, the molecular density of the adsorbed layers increases (whether we visualize additional molecular layers or more completely filled pores), and adsorbate-adsorbate interactions become more significant. The same result would be expected from an increase in the pressure of the system. Thus the system would tend toward the vapor-liquid equilibrium condition which in these cases is oxygen rich. How far the system moves depends on the temperature, the pressure, and the physical limitations of the adsorbent (i.e., the number of molecules that can be accommodated within the pores or on the surface). If the process can proceed sufficiently far, an azeotrope would be formed. The possibility of azeotropes in the oxygen-nitrogen and oxygen-carbon monoxide systems could also be surmized from the crossing of the isotherms at -200 °F or the crossing of the isobars at 760 mmHg. To date no such azeotropes have been reported.

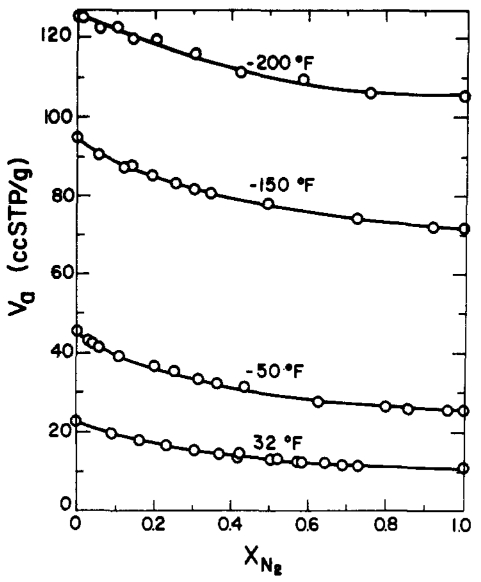

Figure 5. Total volumes adsorbed from nitrogen-carbon monoxide mixtures on molecular sieve type 10X at 760 mmHg.

In the case of the carbon monoxide-nitrogen system, the separation increases as the temperature decreases (Figure 4). Here the more volatile component, nitrogen, is also less strongly adsorbed. Thus the condensed phases in both adsorption equilibria and vapor-liquid equilibria tend to be carbon monoxide rich. As the temperature decreases, the proportion of carbon monoxide in the condensed phase would be expected to increase, and one would not anticipate the formation of an azeotrope for this system.

The total volume adsorbed is, of course, a much stronger function of temperature than the separation. In Figure 5 the volume of the adsorbed mixtures is given as a function of the adsorbed-phase composition. Again the data of Danner and Wenzel (*1*) have been included. This figure is typical of all three binary systems.

Glossary

b	energy parameter in the Langmuir equation
P	total adsorption pressure
T	temperature
V_a	total volume adsorbed in standard cm^3 per g of adsorbent
V_m	monolayer volume parameter of Langmuir equation
X_i	mol % of component i in the adsorbed phase
Y_i	mol % of component i in the vapor phase

Literature Cited

(1) Danner, R. P.; Wenzel, L. A. *AIChE J.* **1969**, *15*, 515.
(2) Dorfman, L. R.; Danner, R. P. *AIChE Symp. Ser.* **1975**, *71*, 30.
(3) Danner, R. P. Ph.D. Thesis, Lehigh University, Bethlehem, PA, 1966.
(4) Joyner, L. G.; Weinberger, E. B.; Montgomery, C. W. *J. Am. Chem. Soc.* **1945**, *67*, 2182.

Received for review August 21, 1980. Accepted December 22, 1980. Financial support of the National Science Foundation (Grant No. GK-18631) is gratefully acknowledged.